Science of the Total Environment 690 (2019) 565–572

Contents lists available at ScienceDirect

Science of the Total Environment

journal homepage: www.elsevier.com/locate/scitotenv

Sorption properties of hydrophobic organic chemicals to micro-sized polystyrene particles

Wei Lin [a], Ruifen Jiang [b,*], Jiayi Wu [a], Songbo Wei [a], Li Yin [a], Xiaoying Xiao [a], Sizi Hu [a], Yong Shen [a,*], Gangfeng Ouyang [a,c]

[a] KLGHEI of Environment and Energy Chemistry, School of Chemistry, Sun Yat-sen University, Guangzhou 510275, China
[b] Guangdong Key Laboratory of Environmental Pollution and Health, School of Environment, Jinan University, Guangzhou 510632, China
[c] College of Chemistry & Molecular Engineering, Center of Advanced Analysis and Computational Science, Zhengzhou University, Zhengzhou 450001, China

HIGHLIGHTS

- The sorption properties of HOCs on the micro-sized PS were investigated.
- An absorption mechanism was verified through theoretical analysis.
- The diffusion of HOCs in the boundary layer on the PS was the dominating process.

GRAPHICAL ABSTRACT

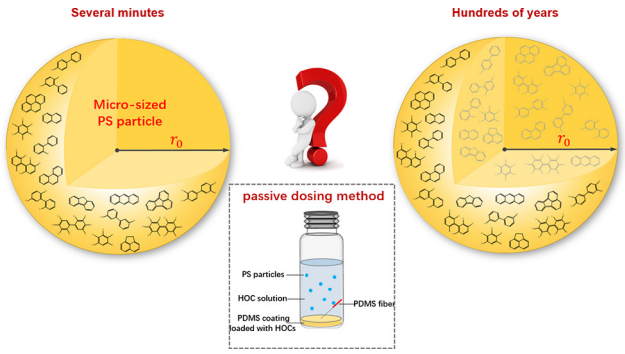

ARTICLE INFO

Article history:
Received 7 May 2019
Received in revised form 28 June 2019
Accepted 30 June 2019
Available online 2 July 2019

Editor: Jay Gan

Keywords:
Microplastics
Polystyrene
Hydrophobic organic chemicals (HOCs)
Sorption properties
Absorption mechanism

ABSTRACT

It has been reported that microplastics (MPs) have strong affinity for hydrophobic organic chemicals (HOCs) and can be ingested accidentally by aquatic organisms, posing a potential threat to the environment. To date, the sorption data used in modelling to clarify the mechanism were mostly obtained in varied sampling durations and regions from different works, which might cause inevitable deviation in modelling results. The current study aimed to illustrate the sorption properties of HOCs to the micro-sized polystyrene (PS). The sorption behaviors of HOCs to the PS were investigated at a certain pre-equilibrium status, and the theoretical analysis was taken into consideration. A bottle-shaped passive dosing system was designed to measure the concentration ratio of HOCs in different phases of the exposure suspension at a certain time ($\log a_{MP}$), including polycyclic aromatic hydrocarbons (PAHs) and polychlorinated biphenyls (PCBs) with $\log K_{ow}$ ranging from 3.17 to 10.20, between water and PS MPs with different dimensions (diameters of 100 nm, 1 μm and 2 μm, respectively).

The calculated $\log a_{MP}$ ranged from 3.73 to 8.34, and a positive correlation was found between $\log a_{MP}$ and $\log \frac{1}{r_0}$ (r_0 is the MP radius). The results indicated that HOCs would diffuse into the PS particles, but the mass transfers inside the particles were slow and would be negligible in some environmental cases. Under theoretical considerations, the diffusion through the boundary layer of the particle was considered as the dominating process because

* Corresponding authors.
E-mail addresses: jiangrf5@jnu.edu.cn (R. Jiang), cessy@mail.sysu.edu.cn (Y. Shen).

https://doi.org/10.1016/j.scitotenv.2019.06.537

it was fast, and the contributions of absorbed amounts on the particle surface were larger for smaller PS particles (*i.e.* 100-nm PS). This study could provide applicable data for further exploring the effects of micro-sized plastics on the HOCs in environmental samples.

1. Introduction

Plastic debris of a multitude of colors and sizes has been identified in marine ecosystems around the world (Blettler et al., 2017; Cheung and Fok, 2017; O'Hanlon et al., 2017; Wilcox et al., 2015). Under the action of external factors such as ultraviolet light (Song et al., 2017; Weinstein et al., 2016), mechanical friction (Brandon et al., 2016) and microbiological activity (Krueger et al., 2015; Skariyachan et al., 2017; Tascioglu et al., 2016), the plastic debris could break down into microplastics (MPs) which have at least one dimension less than millimeters (Rocha-Santos and Duarte, 2015; Ryan et al., 2009). MPs have been reported to be much more harmful than the original-sized plastics because of their extensive distribution (Besseling et al., 2017b; Zhang et al., 2017), large specific surface area (Liu et al., 2016; Zhan et al., 2016) and potential bioaccumulative effect (Canesi et al., 2016, 2015; Grigorakis et al., 2017; Holland et al., 2016).

In natural waters, MPs would sorb various kinds of chemicals, such as polycyclic aromatic hydrocarbons (PAHs) (Rochman et al., 2013a, 2013b; Yuan et al., 2016), polychlorinated biphenyls (PCBs) (Beckingham and Ghosh, 2017; Rochman, 2018), pesticides (Van et al., 2012; Worm et al., 2017), pharmaceuticals and personal care products (PCCPs) (Li et al., 2018; Xu et al., 2018a, 2018b), and heavy metals (Holmes et al., 2012; Turner and Holmes, 2015). Due to their high hydrophobicity, hydrophobic organic chemicals (HOCs) received great attention. It has been reported that the enriching ability of HOCs in the plastic was very strong and the concentration of HOCs in the plastics could be up to 10^6 times that of the surrounding water (Wilcox et al., 2015). The enriching ability of MPs was comparable with that of organic matter (*i.e.*, natural organic matter; Koelmans et al., 2016). Besides, MPs might be much easier to be accidentally ingested by biota compared to other substances such as dissolved organic matters or soil particles. Ory et al. (2017) studied the selectivity for food-*versus*-plastic for *Decapterus muroadsi* and found a selective ingestion of blue MPs by fish. The mean size of the blue particles was similar to that of the blue copepods which were a major food source for the fish. Moreover, with strong sorption and penetration properties, MPs have been found with toxic effects on cells and circulatory systems of organisms (Lin et al., 2019a, 2019b; Nolte et al., 2017; Wegner et al., 2012). Several studies have proved that the sorbed pollutants were able to subsequently transfer to organisms, so MPs were regarded as potential 'vectors' capable of altering the environmental behaviors and biological toxicity of HOCs (Hartmann et al., 2017; Velez et al., 2018). Like many other environmental contaminants, a theoretical understanding of the interaction between HOCs and MPs is mandatory for further exploring the exact risk of MPs in environmental waters (Z. Wang et al., 2018).

It has been reported that the pollutants in the MPs would exchange with the surrounding media, and MPs could be transported to remote waters and deep seas to affect a larger variety of organisms (Rochman et al., 2013a, 2013b; Zarfl and Matthies, 2010). The sorption behaviors of pollutants on MPs were related to plastic types, colors, crystallinity, specific chemical affinities and sizes. Especially, particle size might be one of the most dominant factors among others (Velez et al., 2018; F. Wang et al., 2018). At present, the sorption coefficients of homogeneous chemicals were collected before being fitted with a proposed model in some studies (Dole et al., 2006). Because the data were collected in different sampling durations or regions, they might have inevitable deviations in modelling results. Therefore, to clarify the sorption properties for HOCs to MPs, it would be better to obtain a branch of experimental data and take them into the model consideration.

In this study, the sorption of HOCs to the micro-sized polystyrene (PS) was studied by investigating the sorption behaviors of 7 polycyclic aromatic hydrocarbons (PAHs) and 11 polychlorinated biphenyls (PCBs) with logK_{ow} ranging from 3.17 to 10.20 to polystyrene particles with 3 different diameters (100 nm, 1 μm, 2 μm). A bottle-shaped passive dosing system was employed to generate freely dissolved HOCs of constant concentrations, so as to simplify the analytical process without phase separation. A sorption hypothesis was proposed and discussed based on the experimental data. This study could provide applicable sorption data for short-term biological experiments, and the thoughts for studying the sorption mechanism of HOCs with high hydrophobicity to micro-sized PS particles.

2. Materials and methods

2.1. Materials and instruments

Eighteen unsubstituted HOCs (Table S1) were divided into three groups. The first one was the PAHs group which included naphthalene, acenaphthene, fluorene, phenanthrene, anthracene, fluoranthene and pyrene. The second one was the PCBs group, including PCB-1, 3, 9, 11, 18, 77, pentachlorobenzene (QCB) and hexachlorobenzene (HCB). The last one was the heavy PCBs group, including PCB-136, 194, 209. The PAHs and the micro-sized PS particles with dimensions of 100 nm, 1 μm and 2 μm were purchased from Aladdin (Shanghai, China), while the PCBs were purchased from J&K Scientific Ltd. (Shanghai, China). A SYLGARD 184 silicone elastomer kit purchased from Dow Corning (Shanghai, China) was used to prepare passive dosing vials. Polydimethylsiloxane (PDMS) fibers (i.d. 212 μm, o.d. 300 μm) were purchased from PermSelect (Ann Arbor, MI, USA) and stainless-steel wires (250 μm in diameter) were purchased from Vita Needle Co. (Needham, MA, USA).

For separation and quantification purposes, a 5977A MS (CA, USA) was coupled to an Agilent 7890B GC equipped with a standard split/splitless injector and a fused-silica column (HP-5MS, 30 m length × 0.25 mm I.D. × 0.25 μm thickness). Helium was used as the carrier gas. The injector temperature was set at 280 °C. The oven temperature program was started at 80 °C, at a rate of 20 °C min^{-1} to reach 280 °C, and then held for 10 min at the end. A Selected Ion Mode (SIM) was applied to all HOCs, and their selected ion values were listed in Table S1. A GERSTEL Multi-Purpose System (MPS) was used for the automation process (Mülheim an der Ruhr, Germany).

2.2. The passive dosing method and its working principle

The passive dosing vials were prepared for determining the concentrations of HOCs in different phases of the exposure suspension of HOCs. The preparation procedures were detailed in our previous work (Fig. S1; Jiang et al., 2018). Briefly, a layer of PDMS was coated on the bottom of a 20-mL vial. Then the layer was loaded with different groups of HOCs by adding into the vial a 1-mL standard solution (25 mg L^{-1}, dissolved in methanol), and the vial was put into incubation for 48 h at a constant agitation rate (200 rpm). Next, ultra-pure water (1, 2, 3, 4 and 5 mL, respectively) was added into the dosing vials every 24 h of agitation to increase the loaded amount of HOCs in the PDMS layer. The working principle of the passive dosing method was based on the difference

between the solubility of HOCs in methanol and water. Afterwards, the suspensions were discarded and the vials were cleaned by methanol and ultra-pure water twice (30 s per time) to obtain the final HOCs-loaded vials.

The HOCs-loaded vials were filled with 15 mL of exposure suspensions with different concentrations of PS particles. The PDMS fibers (Lin et al., 2018) were used to monitor the freely dissolved concentrations of HOCs in the suspensions which contained 0.05% NaN_3 as a microorganism inhibitor at room temperature (25 ± 1 °C) for different periods of time. Details were shown in Table S2. After exposure, a liquid-liquid microextraction was conducted to quantify the HOCs in the suspensions. Specifically, 5 mL of the exposure suspensions was transferred to a 10-mL vial, and then 1 mL of hexane containing 100 μg L^{-1} deuterated compounds (See Section 2.4) as the surrogate standard was added to the vial. Then it was sonicated for 30 min and agitated in a rotation agitator at 250 rpm for 24 h. The upper solution layer was transferred to a 2-mL vial for GC–MS analysis. Similarly, the PDMS fiber was directly removed from the exposure suspension with a tweezer and rinsed with ultra-pure water for 30 s. Then it was dried with a piece of Kimwipes and placed in a 200-μL inert tube containing 150 μL of hexane with the surrogate standards. Each inert tube was fixed in a 2-mL vial and agitated at 250 rpm for 24 h before the extraction solution in it was analyzed. Considering that extraction amount and equilibrium time for the 3 groups were different, experimental conditions such as lengths of the fiber coatings, PDMS amounts of the vials and concentration ranges of the PS particles were set respectively for different groups based on preliminary experiments (Table S2).

According to the fundamentals of the passive dosing method, the concentrations of HOCs in different phases of the exposure suspension can be described by the following equation (Gouliarmou et al., 2012):

$$\frac{C_{solution}}{C_{water}} = \frac{C_{bound}}{C_{water}} \times C_{MP} + 1 = a_{MP} \times C_{MP} + 1 \quad (1)$$

where $C_{solution}$ (g L^{-1}) is the total concentration of HOCs in a MP-containing suspension, which can be obtained by liquid-liquid microextraction with hexane as the extractant. C_{water} (g L^{-1}) is the concentration of HOCs in a solution without MPs, which equals to the water concentration in the dosing vial without MP-suspension; C_{bound} (g L^{-1}) is the concentration of HOCs bound to the MP, which equals to the amount of HOC (g) on the MP divided by the amount of MP (kg) in the suspension; C_{MP} (kg L^{-1}) is the concentration of MPs in water. a_{MP} (L kg^{-1}) is defined as the concentration ratio of bound compound and freely dissolved compounds ($\frac{C_{bound}}{C_{water}}$) and can be obtained from the slope of the linear curves by fitting $\frac{C_{solution}}{C_{water}}$ with C_{MP}. When the exposure time is long enough and the sorption process reaches equilibrium, a_{MP} equals the equilibrium sorption coefficient K_{MP}.

2.3. Sorption time profiles of naphthalene to PS particle

The sorption time profiles of naphthalene between water and the PS particle with diameters of 100 nm and 2 μm were obtained using the passive dosing method. In a passive dosing vial containing an MP suspension, there were freely dissolved and MP-bound naphthalene. The pre-loaded naphthalene was released from the PDMS layer into water, and then sorbed by the PS particle. In this process, the free concentration (C_{free}) of naphthalene in the aqueous suspension remained constant. First, the vials were dosed with naphthalene. Then, the suspensions with PS particles (concentrations were 50 mg L^{-1} for the 100-nm PS particles and 75 mg L^{-1} for the 2-μm PS particles) were incubated in the dosing vials for 0.5, 1, 3, 7, 15, 20, 30 days. After that, the concentrations of naphthalene in the exposure suspensions were analyzed. The sorption time profile was obtained by measuring the total concentration ($C_{solution}$) of naphthalene in the suspension after different periods of exposure time.

2.4. Data analysis and quality control

In the current study, all analytical data were subject to strict quality control procedures. For all the compounds, the correlation coefficients of calibration curves obtained from GC–MS were higher than 0.99, and calibration solutions were injected periodically (about every 12 sample injections) to ascertain the stability of the instrument. To analyze the exposure suspensions and the PDMS fibers, deuterated compounds including anthracene, fluoranthene and PCB-77 were used as the surrogate standards to monitor the extraction recoveries of three-ringed, four-ringed PAHs and PCBs/heavy PCBs groups, respectively. Each experimental treatment was conducted in triplicate. The average recoveries of the surrogate standards for different HOCs groups in the suspensions and fibers were listed in Table S3. The stability of the passive dosing vials was monitored by the PDMS fibers in them, measured the freely dissolved concentrations of HOCs in the suspensions. The relative standard deviation (RSD%) data of the fiber-extracted amounts were listed in Table S3, ranging from 7.0% to 16%.

3. Results and discussion

3.1. Sorption of PAHs and PCBs to the PS particles

According to Eq. (1), the linearity of $\frac{C_{solution}}{C_{water}}$ *versus* C_{MP} was obtained for all the HOCs in the current experiment (Fig. 1). The a_{MP} values of HOCs after a certain exposure time were calculated and shown in Table 1. The calculated loga_{MP} ranged from 3.73 to 8.34, 3.51 to 6.59, and 2.66 to 6.39 for the 100-nm, 1-μm and 2-μm PS particles, respectively. In general, for the PS particle with a specific diameter, the loga_{MP} increased as the molecular weight (MW) of the HOCs increased; for an individual HOC, the loga_{MP} decreased as the diameters of the PS particle increased.

Traditionally, K_{ow} is a key parameter to evaluate the enriching ability of a chemical between two media. There was a significant correlation between logK_{ow} and loga_{MP} (Fig. 2). Besides, a linear correlation was observed between the PS particle size and a_{MP} (discussed hereinafter). Therefore, a hypothesis was raised that the absorption process might not reach equilibrium within the current exposure time.

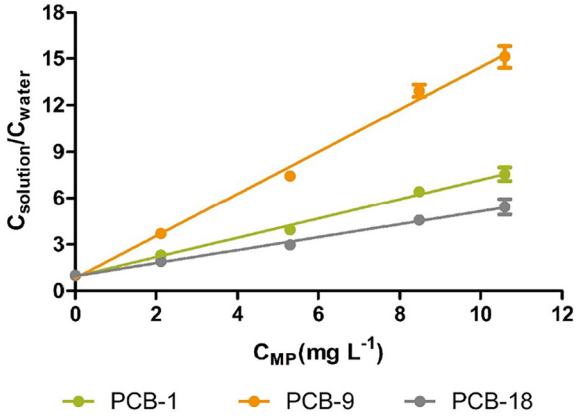

Fig. 1. Sample fitting curves of $\frac{C_{solution}}{C_{water}}$ and C_{MP} for PCB-1,9,18 in 100-nm PS suspensions. All the fitting coefficients for HOCs in MP-containing suspensions with 3 diameters (100 nm, 1 μm, 2 μm) were listed in Table S4. Data were the mean ± SD ($n = 3$). The curves were fitted by the Eq. (1).

Table 1
$\log a_{MP}$ (L kg^{-1}) of HOCs to the PS particle with different diameters.

Chemicals	$\log a_{MP}$ (L kg^{-1})			$\log K_{ow}$[a]	MW	Exposure time/days
	100 nm	1 μm	2 μm			
Naphthalene	3.74	3.51	2.66	3.17	128.2	15
Acenaphthene	5.08	4.33	3.73	4.15	154.2	
Fluorene	5.10	4.57	3.95	4.02	166.2	
Phenanthrene	5.32	4.62	4.00	4.35	178.2	
Anthracene	5.52	4.94	4.33	4.35	178.2	
Fluoranthene	5.12	4.56	4.00	4.93	202.3	
Pyrene	4.92	4.37	3.81	4.93	202.3	
PCB-1	5.79	4.98	4.56	4.40	188.7	30
PCB-3	6.32	5.54	5.15	4.40	188.7	
PCB-9	6.13	5.36	4.97	5.05	223.1	
PCB-11	6.56	5.77	5.40	5.05	223.1	
PCB-18	5.62	5.15	4.82	5.69	257.6	
PCB-77	5.95	5.01	4.72	6.34	292.0	
QCB	6.08	5.34	4.93	5.22	250.3	
HCB	5.80	5.14	4.79	5.86	284.8	
PCB-136	6.70	5.86	5.45	7.62	360.9	100
PCB-194	8.34	7.51	7.28	8.91	429.8	
PCB-209	7.37	6.59	6.39	10.20	498.7	

[a] Estimated by EPI Suite.

3.2. Sorption time profiles of naphthalene to the PS particle

Sorption time profiles of naphthalene were conducted to test the hypothesis. Since the MW of the naphthalene was the smallest among the selected HOCs, its diffusion coefficient should be the biggest and the equilibrium time shortest. As shown in Fig. 3, the amount of naphthalene sorbed to the 100-nm PS particles was higher than that to the 2-μm counterparts during the exposure period. When a one-phase association equation was used to fit the experimental data, the sorption equilibrium time was 3.5 days and 6.5 days, and the sorption equilibrium amounts were 550 ± 5.63 and 296 ± 6.63 pg g^{-1} PS particles for the 100-nm and the 2-μm PS particles, respectively. However, when the sorption time profile of naphthalene was closely investigated in a 2-μm PS suspension, the sorption amount for 30 days was slightly higher than that for 20 days, and the fitting result with one-phase association was not satisfactory as well. Therefore, a two-phase association model was used to fit the experimental data (Fig. 3). The fitting coefficient was 0.93 for the 2-μm PS particles, which was much better than that of the one-phase association model ($R^2 = 0.76$). A similar result was observed for the 100-nm PS particles. The two-phase association model indicated that the sorption equilibrium time for naphthalene on the 2-μm PS particles should be much longer than 30 days, which agreed with the literature (Hüffer and Hofmann, 2016). The results (Fig. 3) also revealed that there were two sorption stages for the HOCs transporting from the aquatic phase to the PS particles, and that the fast sorption stage was much faster than the slow one. The fast kinetic values (k_{fast}) were 2.46 ± 0.21 d^{-1} and 1.76 ± 0.17 d^{-1}, while the slow ones (k_{slow}) were 0.09 ± 0.03 d^{-1} and 0.01 ± 0.00 d^{-1} for the 100-nm and the 2-μm PS particles, respectively.

3.3. Sorption properties of HOCs on PS particles

Based on the results above, a sorption model was applied to explore the sorption mechanism of HOCs on the PS particle. Theoretically, the sorption process of HOCs in MP-contained water can be represented in Fig. 4. The freely dissolved HOCs first diffuse through the static boundary layer around the PS particle. Then they sorb on the particle surface by chemical potential, and further diffuse toward the center of PS particle. In this sorption process, the total transfer velocity of HOCs is determined by its passage through the boundary layer and the particle *per se*, and the total weighted transfer velocity can be expressed as follows (Schwarzenbach et al., 2001):

$$\frac{1}{v_{tot}} = \frac{1}{v_A} + \frac{K_{A/B}}{v_B} \quad (2)$$

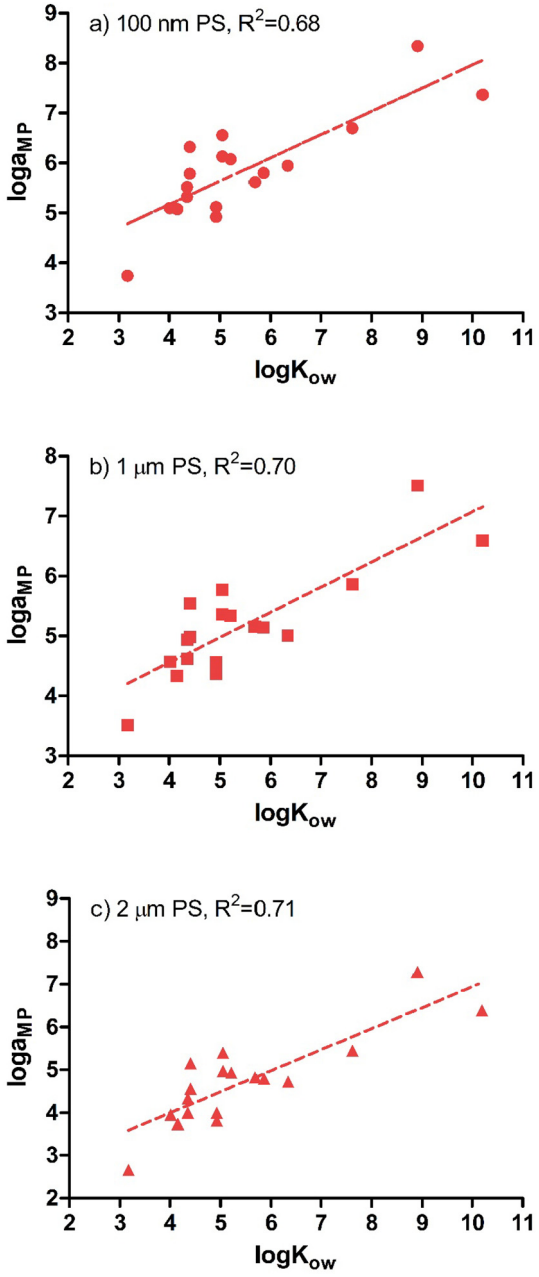

Fig. 2. Correlation between K_{ow} and a_{MP} for the HOCs in water containing a) 100-nm PS, b) 1-μm PS, c) 2-μm PS, respectively. The correlation coefficients (R^2) in the figures indicated a significant correlation between K_{ow} and a_{MP}.

$$v_A = \frac{D_{PS}}{r} \quad (3)$$

$$v_B = \frac{D_{water}}{\delta} \quad (4)$$

where v_{tot} is the total weighted transfer velocity for the sorption process (cm s^{-1}). v_A and v_B are the transfer velocities across the PS particle and the boundary layer, respectively (cm s^{-1}). $K_{A/B}$ is the sorption coefficient of the analyte between the PS particle and water at equilibrium. D_{PS} and D_{water} are the diffusion coefficients of the analyte in the PS particle and the boundary layer, respectively. r is the radius of the PS particle, and δ is the thickness of the boundary layer adhered to the particle.

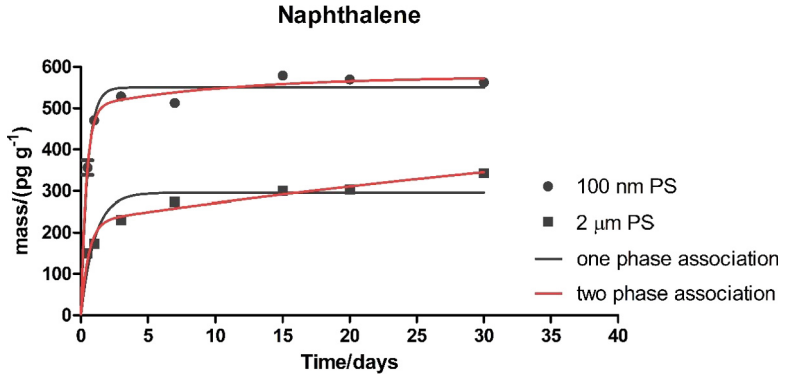

Fitting model	Fitting value	100-nm PS particle	2-μm PS particle
One-phase association[1)]	Equilibrium amount/pg g^{-1}	550±5.63	296±6.63
	kinetic value (k) /d^{-1}	2.03±0.11	0.96±0.10
	Fitting coefficient (R^2)	0.84	0.76
Two-phase association[2)]	Equilibrium amount/pg g^{-1}	577	577
	Fast kinetic value (k_{fast})/d^{-1}	2.46±0.21	1.76±0.17
	Slow kinetic value (k_{slow}) /d^{-1}	0.09±0.03	0.01±0.00
	Span fast (S_{fast})/pg g^{-1}	503	226
	Span slow (S_{slow})/pg g^{-1}	74.5	352
	Percentage of slow/%	12.9±2.77	60.9±1.23
	Fitting coefficient (R^2)	0.89	0.93

[1)] One-phase association: $m = m_0 + (m_{eq} - m_0) \cdot (1 - e^{-kt})$

[2)] Two-phase association: $m = m_0 + S_{fast}(1 - e^{-k_{fast}t}) + S_{slow}(1 - e^{-k_{slow}t})$

Fig. 3. Sorption time profiles for naphthalene in pure water with PS particles of different sizes. Data are the mean ± SD ($n = 3$). The one-phase curves were fitted using the first-order association equation: $q_f = q_0 + Ae^{at}$; The two-phase curves were fitted using the two-phase association equation: $q_f = q_0 + S_{fast} \cdot (1 - e^{-k_{fast}t}) + S_{slow} \cdot (1 - e^{-k_{slow}t})$.

(1) When $\frac{1}{v_A} \gg \frac{K_{A/B}}{v_B}$, Eq. (2) can be simplified as $v_{tot} = v_A$, indicating that the transfer velocity in the boundary layer is much faster than that in the PS particle. The transfer in the PS particle should be the rate-limiting step that dominates the speed of the sorption process.

(2) When $\frac{1}{v_A} \ll \frac{K_{A/B}}{v_B}$, Eq. (2) can be simplified as $v_{tot} = \frac{v_B}{K_{A/B}}$, indicating that the velocity of the whole sorption process mainly depends on the transfer of the analyte through the boundary layer.

As reported, for the HOCs with MW ranging from 128 to 497, the diffusion coefficients (D) were from 10^{-15} to 10^{-26} cm^2 s^{-1} in the PS particle; while in water, the diffusion coefficients were about 10^{-6} cm^2 s^{-1} for all the HOCs (Dole et al., 2006). According to the empirical equations, the thickness of the boundary layers for the 100-nm and the 2-μm PS particles in the current exposure condition were estimated to be 24 μm and 479 μm, respectively (detailed calculation process was in Text S1). Therefore, $\frac{1}{v_A}$ and $\frac{K_{A/B}}{v_B}$ could be estimated by Eqs. (3) and (4) when considering the concentrations of HOCs in different phases of the exposure suspension ($\log a_{MP}$ ranging from 3.74 to 8.34 L kg^{-1} in this study) instead of the equilibrium sorption coefficients, $K_{A/B}$. It was measured previously that HOC concentrations in plastic particles and those in organic matters or in lipids of organisms were often of comparable orders of magnitude (Endo et al., 2013; Lee et al., 2014; Liu et al., 2016; Site, 2001). Therefore, although the $K_{A/B}$ was substituted by $\log a_{MP}$, the results indicated that $\frac{1}{v_A} \gg \frac{K_{A/B}}{v_B}$ should be the case in the current study, where the transfer velocity of HOCs in the PS particle was the rate-limiting step in the sorption process.

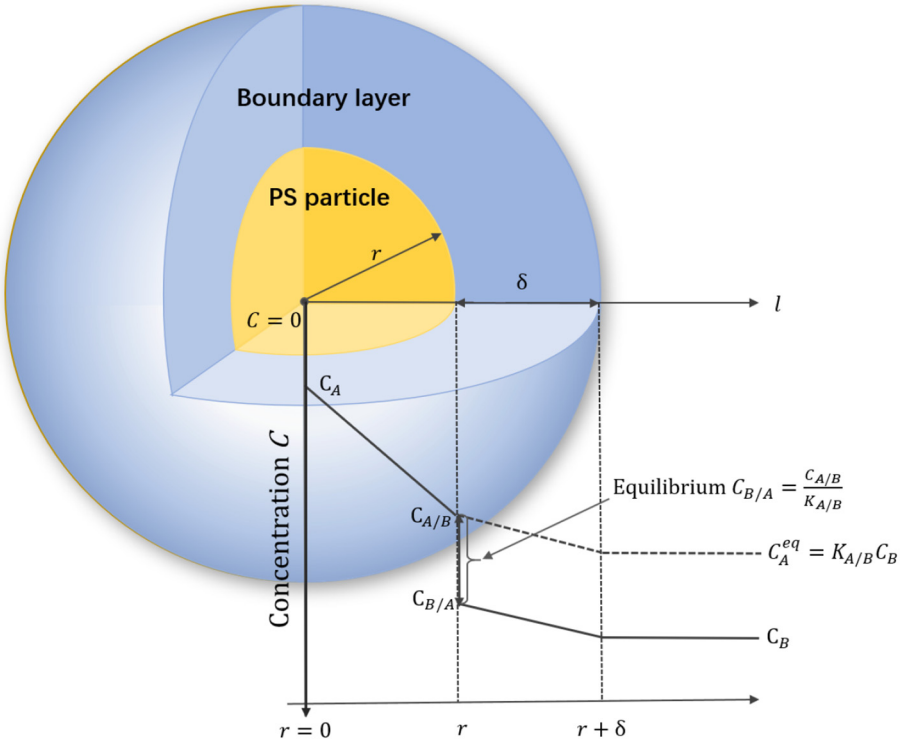

Fig. 4. A schematic diagram for mass transfer of analytes through the boundary layer and the PS particle at partition equilibrium (whose shape is spherical; Fig. S2).

According to the diffusion law by Einstein, diffusion is the net movement of a molecule across the boundary layer on the surface of the PS particle. The diffusion time (t) of a molecule through a polymer for a distance, *l*, can be estimated by (Crank, 1979):

$$t = \frac{l^2}{6D} \tag{5}$$

when *l* is the radius of the PS particle, the diffusion time of naphthalene through the 100-nm and the 2-μm PS particles was about 2.9 h and 48.5 days, respectively. *D* is the diffusion coefficient of the chemical in specific material, which can be read from literature. This result further proved that naphthalene did not reach equilibrium within 30 days' exposure (Fig. 3). Based on this theory, the estimated diffusion time for pyrene, PCB-11, PCB-18 to transfer through the 100-nm PS particles was 4.8 days, 22.0 days and 215.4 days, respectively. Only the HOCs with MW smaller than 223.1 g mol^{-1} (PCB-11) reached equilibrium in the 100-nm PS particles in our experiment. The results verified that it was the absorption mechanism underlying the sorption process between HOCs and the PS particles. The sorption process included two stages: the fast sorption stage for the HOCs diffusing through aqueous boundary layer; and the slow one for the HOCs penetrating inside the PS particle. For most of the biological experiments, the exposure time was relatively short. Only the HOCs absorbed on the particle surface were able to be released and therefore affect bioaccumulation. It could be simplified as the sorption process on the surface of the PS particle, because most of the HOCs only stayed on the surface or diffused a few nanometers inside the particle. All the estimated equilibrium time was listed in Table S5.

3.4. Fast sorption and slow sorption process

Such understandings have been proposed for the sorption processes between the chemicals and particles. For example, the sorption of the wastewater pollutants to 260-μm polyethylene was conceptualized as consisting of two simultaneous process: mass transfer and intraparticle diffusion (Seidensticker et al., 2017). Similar findings were also applied to the sorption of the low-polarity organic chemicals to natural soil particles (Xia and Ball, 1999), the desorption of brominated flame retardants from MPs (Sun et al., 2019), the diffusion of polybrominated diphenyl ethers (PBDE) in low density polyethylene (LDPE) (Baek et al., 2016). Because the diffusion coefficients of HOCs in the PS particle were small, the time for HOCs to diffuse through the boundary layer was much shorter than that to penetrate into the PS particle. For instance, it only took seconds and minutes for naphthalene to cross through the boundary layer with the thickness of 24 μm (100-nm PS) and 479 μm (2-μm PS), respectively. For the HOCs which were more hydrophobic than naphthalene, the mass transfer kinetics should be slower (Lin et al., 2018). Besides, particle size played an important role on the relative contributions of the two stages respectively. For example, the absorbed naphthalene on the surface of the particles contributed about 87.1% of the equilibrium accumulation amounts for the 100-nm PS, while only 39.1% for the 2-μm PS, respectively (Fig. 2).

Because MPs are small in size, it is easy to be ingested and excreted by organisms during the exposure period. The gut retention time of MPs were usually in the range of several minutes to a few days (Bakir et al., 2016; Besseling et al., 2017a; Cole et al., 2016; Koelmans et al., 2013). Therefore, in the biological experiments, the absorbed part of HOCs on the surface of the PS particle is more bioavailable than that diffusing into the particle. The fast sorption process is the mass transfer of the HOCs absorbed to the surface of the PS particle (or a few nanometers in depth). Also, there is a relationship between the sorption coefficient expressed by volume (K_{MP}^{V}) and surface area (K_{MP}^{s}). Therefore, the absorption amounts should be proportional to the surface area of the particles. Based on this correlation, the absorbed amounts of the fast process can be indirectly evaluated for PS particles with different sizes.

In the current study, the shapes of all the PS particles were spherical (Fig. S2). In theory, the relationship between sorption coefficient expressed by volume (K_{MP}^{V}) and surface area (K_{MP}^{s}) can be described by the following equations (McMurry, 2003):

$$K_{MP}^{V} = \frac{C_{bound}}{C_{water}} = \frac{n_{bound}/V_{MP}}{C_{water}} = \frac{n_{bound}/S_{MP}}{C_{water}} \times \frac{3\gamma}{r_0} = K_{MP}^{s} \times \frac{3\gamma}{r_0} \tag{6}$$

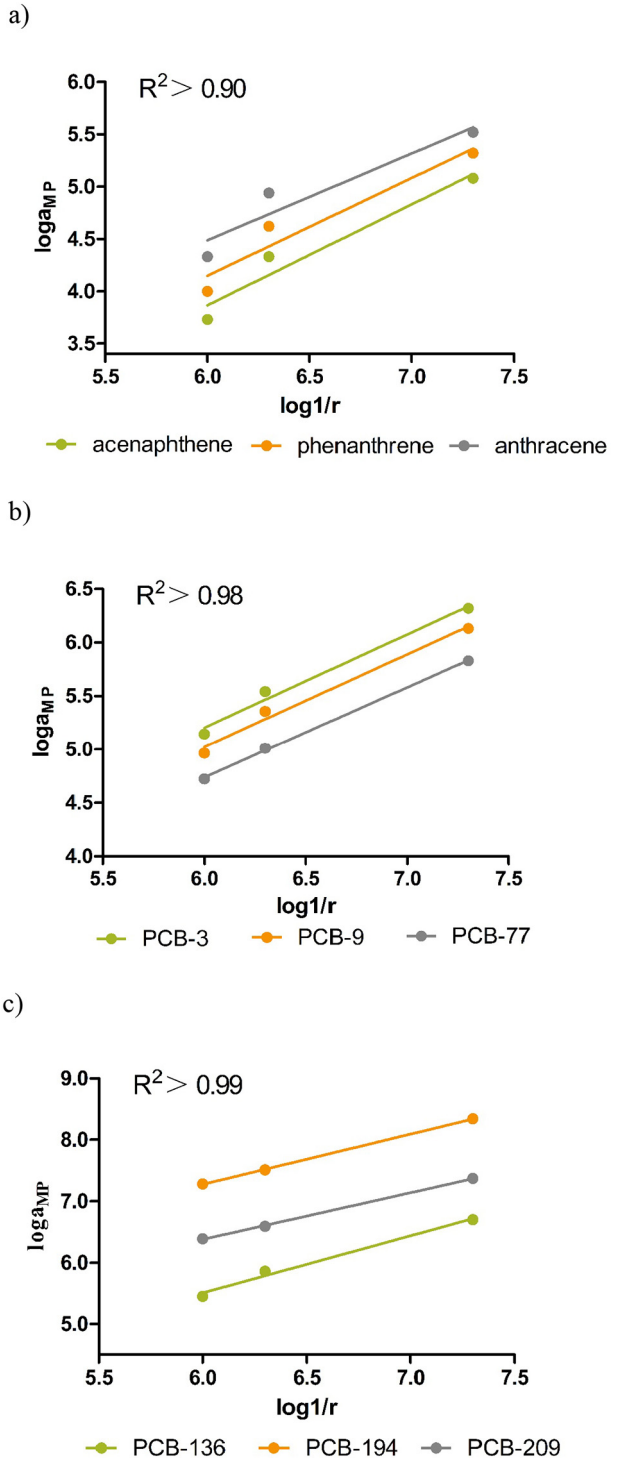

Fig. 5. Fitting curves of $\log a_{MP}$ and $\log\frac{1}{r_0}$ based on Eq. (7) for some HOCs (take 3 of each group as examples).

$$\log K_{MP}^{V} = \log K_{MP}^{s} + \log 3\gamma + \log\frac{1}{r_0} \quad (7)$$

where K_{MP}^{V} and K_{MP}^{S} are the sorption coefficients calculated by volume and surface area of a plastic particle, respectively. n_{bound} is the amount of bound substance per unit volume of the MPs. V_{MP} and S_{MP} are the volume and surface area for a single plastic particle, respectively. r_0 is the radius of the particle and γ is the parameter that represents the roughness of the particle's surface. For a sorption process on the surface of the particle, K_{MP}^{s} and γ should be constant, while $\log K_{MP}^{V}$ is linear to $\log\frac{1}{r_0}$. By fitting the obtained data with Eq. (7), acceptable linearity was observed between the $\log a_{MP}$ and $\log\frac{1}{r_0}$ for all HOCs (Fig. 5).

Ernandez (2005) studied the sorption behaviors of several PCB congeners for a PS film in freshwater at 25 °C, and the calculated sorption coefficients of PCB-18 and PCB-77 were $10^{2.49}$ and $10^{2.61}$ L kg^{-1}, respectively. Significant differences were observed when comparing the obtained a_{MP} values of PCB-18 and PCB-77 for the 100-nm PS particles (Table 1) with the ones from Ernandez. However, when the sorption coefficients were expressed by surface area (K_{MP}^{S}) instead of volume, they were calculated as 0.0098 and 0.0113 L·m kg^{-1} for PCB-18 and PCB-77, respectively, in the current work. They were similar to the ones from Ernandez's work (0.0047 and 0.0062 L·m kg^{-1} for PCB-18 and PCB-77, respectively; Ernandez, 2005). The results demonstrated that although the HOCs could penetrate into the PS particle, transferring of HOCs through the boundary layers should be a dominant process in the MP-containing suspensions. The mass transfers in the boundary layers were much faster than those inside the particles. Therefore, the absorbed HOCs on the surface of the PS particle were considered to be bioavailable in the biological experiments, while the penetrated HOCs inside the particle were negligible.

4. Conclusions

This study tested the hypothesis that the sorption properties for HOCs to MPs could be illustrated at pre-equilibrium by a combination of experimental data and theoretical considerations. For the first time, the sorption behaviors of HOCs with a wide range of $\log K_{ow}$ were investigated among micro-sized PS particles at a certain time. Although the HOCs were able to penetrate into the PS particles, the mass transfer rates were extremely slow. The sorption on the surface of the particle was verified as the dominating process through theoretical analysis. Moreover, the contributions of the fast transfer process in the boundary layer and the slow penetration process inside the particle were clarified. The fast transfer process was the dominate one when taking the actual circumstances of biological experiments into account. Since the environmental water is much more complicated, further studies should be conducted to explore the combined effects of different particles on the sorption behaviors of HOCs.

Declaration of Competing Interest

The authors declare no competing financial interest.

Acknowledgements

This research was supported by the projects of the National Natural Science Foundation of China (21777058, 21407184, 21477166, 21527813). In particular, the authors thank Xuekai Xu for the graphical editing and beautification of this article.

Appendix A. Supplementary data

Supplementary data to this article can be found online at https://doi.org/10.1016/j.scitotenv.2019.06.537.

References

Baek, K., Molina, F.J., Allan, I.J., 2016. Implications of observed PBDE diffusion coefficients in low density polyethylene and silicone rubber. Environ. Sci. Process. Impacts 18, 87–94.

Bakir, A., Connor, I.A.O., Rowland, S.J., Hendriks, A.J., Thompson, R.C., 2016. Relative importance of microplastics as a pathway for the transfer of hydrophobic organic chemicals to marine life. Environ. Pollut. 219, 56–65.

Beckingham, B., Ghosh, U., 2017. Differential bioavailability of polychlorinated biphenyls associated with environmental particles: microplastic in comparison to wood, coal and biochar. Environ. Pollut. 220, 150–158.

Besseling, E., Foekema, E.M., Van Den Heuvel-Greve, M.J., Koelmans, A.A., 2017a. The effect of microplastic on the uptake of chemicals by the lugworm *Arenicola marina* (L.) under environmentally relevant exposure conditions. Environ. Sci. Technol. 51, 8795–8804.

Besseling, E., Quik, J.T.K., Sun, M., Koelmans, A.A., 2017b. Fate of nano- and microplastic in freshwater systems: a modeling study. Environ. Pollut. 220, 540–548.

Blettler, M.C.M., Ulla, M.A., Rabuffetti, A.P., Garello, N., 2017. Plastic pollution in freshwater ecosystems: macro-, meso-, and microplastic debris in a floodplain lake. Environ. Monit. Assess. 189, 581.

Brandon, J., Goldstein, M., Ohman, M.D., 2016. Long-term aging and degradation of microplastic particles: comparing in situ oceanic and experimental weathering patterns. Mar. Pollut. Bull. 110, 299–308.

Canesi, L., Ciacci, C., Bergami, E., Monopoli, M.P., Dawson, K.A., Papa, S., Canonico, B., Corsi, I., 2015. Evidence for immunomodulation and apoptotic processes induced by cationic polystyrene nanoparticles in the hemocytes of the marine bivalve *Mytilus*. Mar. Environ. Res. 111, 34–40.

Canesi, L., Ciacci, C., Fabbri, R., Balbi, T., Salis, A., Damonte, G., Cortese, K., Caratto, V., Monopoli, M.P., Dawson, K., Bergami, E., Corsi, I., 2016. Interactions of cationic polystyrene nanoparticles with marine bivalve hemocytes in a physiological environment: role of soluble hemolymph proteins. Environ. Res. 150, 73–81.

Cheung, P.K., Fok, L., 2017. Characterisation of plastic microbeads in facial scrubs and their estimated emissions in Mainland China. Water Res. 122, 53–61.

Cole, M., Lindeque, P.K., Fileman, E., Clark, J., Lewis, C., Halsband, C., Galloway, T.S., 2016. Microplastics alter the properties and sinking rates of zooplankton faecal pellets. Environ. Sci. Technol. 50, 3239–3246.

Crank, J., 1979. The Mathematics of Diffusion. 2nd ed. Oxford University Press Inc., New York.

Dole, P., Feigenbaum, A.E., Cruz, C.D. La, Pastorelli, S., Paseiro, P., Hankemeier, T., Voulzatis, Y., Aucejo, S., Saillard, P., Papaspyrides, C., Dole, P., Feigenbaum, A.E., Cruz, C.D. La, Paseiro, P., Hankemeier, T., Voulzatis, Y., Aucejo, S., 2006. Typical diffusion behaviour in packaging polymers-application to functional barriers. Food Addit. Contam. 23, 202–211.

Endo, S., Yuyama, M., Takada, H., 2013. Desorption kinetics of hydrophobic organic contaminants from marine plastic pellets. Mar. Pollut. Bull. 74, 125–131.

Ernandez, R.U.J.H., 2005. Uptake of polychlorinated biphenyls (PCBs) from an aqueous medium by polyethylene, polyvinyl chloride, and polystyrene films. J. Agric. Food Chem. 53, 164–169.

Gouliarmou, V., Smith, K.E.C., De Jonge, L.W., Mayer, P., 2012. Measuring binding and speciation of hydrophobic organic chemicals at controlled freely dissolved concentrations and without phase separation. Anal. Chem. 84, 1601–1608.

Grigorakis, S., Mason, S.A., Drouillard, K.G., 2017. Determination of the gut retention of plastic microbeads and microfibers in goldfish (*Carassius auratus*). Chemosphere 169, 233–238.

Hartmann, N.B., Rist, S., Bodin, J., Jensen, H.S., Schmidt, S.N., Mayer, P., Meibom, A., Baun, A., 2017. Microplastics as vectors for environmental contaminants: exploring sorption, desorption, and transfer to biota. Integr. Environ. Assess. Manag. 13, 488–493.

Holland, E.R., Mallory, M.L., Shutler, D., 2016. Plastics and other anthropogenic debris in freshwater birds from Canada. Sci. Total Environ. 571, 251–258.

Holmes, L.A., Turner, A., Thompson, R.C., 2012. Adsorption of trace metals to plastic resin pellets in the marine environment. Environ. Pollut. 160, 42–48.

Hüffer, T., Hofmann, T., 2016. Sorption of non-polar organic compounds by micro-sized plastic particles in aqueous solution. Environ. Pollut. 214, 194–201.

Jiang, R., Lin, W., Wu, J., Xiong, Y., Zhu, F., Bao, L.-J., You, J., Ouyang, G., Zeng, E.Y., 2018. Quantifying nanoplastic-bound chemicals accumulated in *Daphnia magna* with a passive dosing method. Environ. Sci. Nano 5, 776–781.

Koelmans, A.A., Besseling, E., Wegner, A., Foekema, E.M., 2013. Plastic as a carrier of POPs to aquatic organisms: a model analysis. Environ. Sci. Technol. 47, 7812–7820.

Koelmans, A.A., Bakir, A., Burton, G.A., Janssen, C.R., 2016. Microplastic as a vector for chemicals in the aquatic environment: critical review and model-supported reinterpretation of empirical studies. Environ. Sci. Technol. 50, 3315–3326.

Krueger, M.C., Harms, H., Schlosser, D., 2015. Prospects for microbiological solutions to environmental pollution with plastics. Appl. Microbiol. Biotechnol. 99, 8857–8874.

Lee, H., Shim, W.J., Kwon, J.H., 2014. Sorption capacity of plastic debris for hydrophobic organic chemicals. Sci. Total Environ. 470–471, 1545–1552.

Li, J., Zhang, K., Zhang, H., 2018. Adsorption of antibiotics on microplastics. Environ. Pollut. 237, 460–467.

Lin, W., Jiang, R., Shen, Y., Xiong, Y., Hu, S., Xu, J., Ouyang, G., 2018. Effect of dissolved organic matter on pre-equilibrium passive sampling: a predictive QSAR modeling study. Sci. Total Environ. 635, 53–59.

Lin, W., Jiang, R., Hu, S., Xiao, X., Wu, J., Wei, S., Xiong, Y., Ouyang, G., 2019a. Investigating the toxicities of different functionalized polystyrene nanoplastics on *Daphnia magna*. Ecotoxicol. Environ. Saf. 180, 509–516.

Lin, W., Jiang, R., Xiong, Y., Wu, J., Xu, J., Zheng, J., Zhu, F., 2019b. Quantification of the combined toxic effect of polychlorinated biphenyls and nano-sized polystyrene on *Daphnia magna*. J. Hazard. Mater. 364, 531–536.

Liu, L., Fokkink, R., Koelmans, A.A., 2016. Sorption of polycyclic aromatic hydrocarbons to polystyrene nanoplastic. Environ. Toxicol. Chem. 35, 1650–1655.

McMurry, J., 2003. Fundamentals of Organic Chemistry. Fifth. ed. Agnus McDonald.

Nolte, T.M., Hartmann, N.B., Kleijn, J.M., Garnæs, J., van de Meent, D., Jan Hendriks, A., Baun, A., 2017. The toxicity of plastic nanoparticles to green algae as influenced by surface modification, medium hardness and cellular adsorption. Aquat. Toxicol. 183, 11–20.

O'Hanlon, N.J., James, N.A., Masden, E.A., Bond, A.L., 2017. Seabirds and marine plastic debris in the northeastern Atlantic: a synthesis and recommendations for monitoring and research. Environ. Pollut. 231, 1291–1301.

Ory, N.C., Sobral, P., Ferreira, J.L., Thiel, M., 2017. Amberstripe scad *Decapterus muroadsi* (Carangidae) fish ingest blue microplastics resembling their copepod prey along the coast of Rapa Nui (Easter Island) in the South Pacific subtropical gyre. Sci. Total Environ. 586, 430–437.

Rocha-Santos, T., Duarte, A.C., 2015. A critical overview of the analytical approaches to the occurrence, the fate and the behavior of microplastics in the environment. TrAC - Trends Anal. Chem. 65, 47–53.

Rochman, C.M., 2018. Microplastics research—from sink to source. Science (80-.) 360, 28–29.

Rochman, C.M., Hoh, E., Hentschel, B.T., Kaye, S., 2013a. Long-term field measurement of sorption of organic contaminants to five types of plastic pellets: implications for plastic marine debris. Environ. Sci. Technol. 47, 1646–1654.

Rochman, C.M., Manzano, C., Hentschel, B.T., Simonich, S.L.M., Hoh, E., 2013b. Polystyrene plastic: a source and sink for polycyclic aromatic hydrocarbons in the marine environment. Environ. Sci. Technol. 47, 13976–13984.

Ryan, P.G., Moore, C.J., van Franeker, J.A., Moloney, C.L., 2009. Monitoring the abundance of plastic debris in the marine environment. Philos. Trans. R. Soc. B Biol. Sci. 364, 1999–2012.

Schwarzenbach, R.P., Gschwend, P.M., Imboden, D.M., 2001. Environmental Organic Chemistry. 2nd ed. John Wiley & Sons, Inc.

Seidensticker, S., Zar, C., Cirpka, O.A., Fellenberg, G., Grathwohl, P., 2017. Shift in mass transfer of wastewater contaminants from microplastics in the presence of dissolved substances. Environ. Sci. Technol. 51, 12254–12263.

Site, A.D., 2001. Factors affecting sorption of organic compounds in natural sorbent/water systems and sorption coefficients for selected pollutants. A review. J. Phys. Chem. Ref. Data 30, 187–439.

Skariyachan, S., Setlur, A.S., Naik, S.Y., Naik, A.A., Usharani, M., Vasist, K.S., 2017. Enhanced biodegradation of low and high-density polyethylene by novel bacterial consortia formulated from plastic-contaminated cow dung under thermophilic conditions. Environ. Sci. Pollut. Res. 24, 8443–8457.

Song, Y.K., Hong, S.H., Jang, M., Han, G.M., Jung, S.W., Shim, W.J., 2017. Combined effects of UV exposure duration and mechanical abrasion on microplastic fragmentation by polymer type. Environ. Sci. Technol. 51, 4368–4376.

Sun, B., Hu, Y., Cheng, H., Tao, S., 2019. Releases of brominated flame retardants (BFRs) from microplastics in aqueous medium: kinetics and molecular-size dependence of diffusion. Water Res. 151, 215–225.

Tascioglu, C., Tufan, M., Yalcin, M., Sen, S., 2016. Determination of biological performance, dimensional stability, mechanical and thermal properties of wood-plastic composites produced from recycled chromated copper arsenate-treated wood. J. Thermoplast. Compos. Mater. 29, 1461–1479.

Turner, A., Holmes, L.A., 2015. Adsorption of trace metals by microplastic pellets in fresh water. Environ. Chem. 12, 600–610.

Van, A., Rochman, C.M., Flores, E.M., Hill, K.L., Vargas, E., Vargas, S.A., Hoh, E., 2012. Persistent organic pollutants in plastic marine debris found on beaches in San Diego, California. Chemosphere 86, 258–263.

Velez, J.F.M., Shashoua, Y., Syberg, K., Khan, F.R., 2018. Considerations on the use of equilibrium models for the characterisation of HOC-microplastic interactions in vector studies. Chemosphere 210, 359–365.

Wang, Z., Chen, M., Zhang, L., Wang, K., Yu, X., Zheng, Z., Zheng, R., 2018a. Sorption behaviors of phenanthrene on the microplastics identified in a mariculture farm in Xiangshan Bay, southeastern China. Sci. Total Environ. 628–629, 1617–1626.

Wang, F., Wong, C.S., Chen, D., Lu, X., Wang, F., Zeng, E.Y., 2018b. Interaction of toxic chemicals with microplastics: a critical review. Water Res. 139, 208–219.

Wegner, A., Besseling, E., Foekema, E.M., Kamermans, P., Koelmans, A.A., 2012. Effects of nanopolystyrene on the feeding behavior of the blue mussel (*Mytilus edulis* L.). Environ. Toxicol. Chem. 31, 2490–2497.

Weinstein, J.E., Crocker, B.K., Gray, A.D., 2016. From macroplastic to microplastic: degradation of high-density polyethylene, polypropylene, and polystyrene in a salt marsh habitat. Environ. Toxicol. Chem. 35, 1632–1640.

Wilcox, C., Van Sebille, E., Hardesty, B.D., 2015. Threat of plastic pollution to seabirds is global, pervasive, and increasing. Proc. Natl. Acad. Sci. 112, 11899–11904.

Worm, B., Lotze, H.K., Jubinville, I., Wilcox, C., Jambeck, J., 2017. Plastic as a persistent marine pollutant. Annu. Rev. Environ. Resour. 42, 1–26.

Xia, G., Ball, W.P., 1999. Adsorption-partitioning uptake of nine low-polarity organic chemicals on a natural sorbent. Environ. Sci. Technol. 33, 262–269.

Xu, B., Liu, F., Brookes, P.C., Xu, J., 2018a. The sorption kinetics and isotherms of sulfamethoxazole with polyethylene microplastics. Mar. Pollut. Bull. 131, 191–196.

Xu, B., Liu, F., Brookes, P.C., Xu, J., 2018b. Microplastics play a minor role in tetracycline sorption in the presence of dissolved organic matter. Environ. Pollut. 240, 87–94.

Yuan, X., Yang, X., Zhang, A., Ma, X., Gao, H., Na, G., Zong, H., Liu, G., Sun, Y., 2016. Distribution, potential sources and ecological risks of two persistent organic pollutants in the intertidal sediment at the Shuangtaizi Estuary, Bohai Sea of China. Mar. Pollut. Bull. 114, 419–427.

Zarfl, C., Matthies, M., 2010. Are marine plastic particles transport vectors for organic pollutants to the Arctic? Mar. Pollut. Bull. 60, 1810–1814.

Zhan, Z., Wang, J., Peng, J., Xie, Q., Huang, Y., Gao, Y., 2016. Sorption of 3,3′,4,4′-tetrachlorobiphenyl by microplastics: a case study of polypropylene. Mar. Pollut. Bull. 110, 559–563.

Zhang, W., Zhang, S., Wang, J., Wang, Y., Mu, J., Wang, P., Lin, X., Ma, D., 2017. Microplastic pollution in the surface waters of the Bohai Sea, China. Environ. Pollut. 231, 541–548.